Layout and Expected Performance of the LHCb TT Station

J. Gassner, M. Needham, O. Steinkamp

December 31, 2003

Abstract

An improved layout for the detection layers of the Trigger Tracker (TT station) is described and estimates are given for the expected signal-to-noise performance of the detector.

1 Introduction

The TT station is located downstream of RICH 1 and in front of the entrance of the LHCb spectrometer magnet. The station consists of four planar detection layers with a width and height of approximately 160 cm and 130 cm, respectively. This amounts to a total active area of approximately $8.4\,\mathrm{m}^2$ to be covered by silicon microstrip detectors. The four detection layers are arranged in two half stations separated by approximately 27 cm along the beam axis. The first two layers (TTa) are centered around $z = 235\,\mathrm{cm}$ downstream of the nominal interaction point, the third and fourth layer (TTb) are centered around $z = 262\,\mathrm{cm}$.

The design of the TT station has been described in the LHCb reoptimization TDR [1]. The layout of the detection layers as presented in the TDR made use of silicon sensors of the same length and width and with the same strip geometry as those employed in the LHCb Inner Tracker [2]. Silicon sensors for the TT station have, however, to be thicker than those employed in the Inner Tracker since they are arranged in longer readout sectors[1]. In order to determine the required sensor thickness for the TT station, prototype ladders from $320\,\mu$m, $410\,\mu$m and $500\,\mu$m thick silicon sensors were constructed and tested in the CERN-X7 test-beam facility [4]. At the time of submission of the TDR, the analysis of the test-beam data had shown that a sensor thickness of at least $410\,\mu$m would be required in order to ensure a fully efficient operation of the TT station.

However, readout strips in the TT station will be longer than those tested on the prototype ladders. It is thus necessary to extrapolate the signal-to-noise performance measured in the test-beam to the strip lengths that are foreseen for the TT station. An extrapolation procedure is described in this note. Applying it to the TDR layout led to the conclusion that the expected performance for $410\,\mu$m thick sensors would be marginal and that $500\,\mu$m thick sensors are required in order to ensure robust operation of the detector.

An improved layout for the TT station using $500\,\mu$m thick silicon sensors is described in Chapter 2. It makes use of silicon sensors of an existing design that has been developed for

[1] Longer readout sectors result in higher readout strip capacitances and a worse noise performance of the front-end readout amplifier. Thicker sensors have to be employed in order to obtain sufficiently high signal-to-noise ratios for efficient operation of the detector.

Table 1: Nominal acceptance of the TT station.

	TTa	TTb
average z position	235.0 cm	262.0 cm
width of sensitive surface	145.4 cm	162.1 cm
height of sensitive surface	120.0 cm	133.8 cm
width of beam pipe hole	7.74 cm	7.74 cm
height of beam pipe hole	7.40 cm	7.40 cm

the outer barrel of the CMS Silicon Tracker. Prototype ladders constructed from this type of sensors have already been tested extensively in laboratory setups [7] and in the CERN-X7 test beam [4].

The expected strip capacitances for the different readout sectors in the improved layout are calculated in Chapter 3. the extrapolation algorithm and the expected signal-to-noise performance of the detector are presented in Chapter 4.

Finally, the results of the extrapolation algorithm as applied to the TDR layout are shown in an Appendix to this note.

2 Layout of Detection Layers

The nominal acceptance of the LHCb detector is 300 mrad in the horizontal bending plane of the spectrometer magnet and 250 mrad in the vertical plane. This translates to the nominal dimensions of the detection layers summarised in Table 1.

Towards small polar angles with respect to the beam axis, the acceptance of the station is limited by the LHC beam pipe that traverses the detector. The dimensions of the square-shaped beam-pipe hole are also quoted in Table 1. They are measured up to the edge of the silicon sensors and take into account the diameter of the beam pipe, the clearance between beam pipe and detector box, the thickness of the detector box, the clearance between detector box and silicon ladders and the dead space due to the ladder support structure. The values listed in Table 1 are based on a more advanced mechanical design of the detector box and thus differ slightly from those quoted in the TDR [1].

The layout described here makes use of 500 μm thick OB2 silicon sensors that have been developed for the Outer Barrel of the CMS silicon tracker [3]. The relevant geometry parameters of these sensors are summarised in Table 2.

The layout for each of the four detection layers is shown in Figure 1. The areas above and below the beam pipe are each covered by a single seven-sensor long silicon ladder, the areas to the left and to the right of the beam pipe are covered by seven (TTa) or eight (TTb) staggered 14-sensor long ladders. Ladders are installed vertically in the first and fourth detection layers, whereas they are individually rotated by a stereo angle of $+5^\circ$ and -5° in the second and third detection layers, respectively.

As in the TDR layout, each ladder is vertically split into several readout sectors, indicated by different shadings in Figure 1. All front-end readout hybrids are located at the top end or the bottom end of a ladder, outside of the acceptance of the experiment. Kapton interconnect cables are employed to connect the three-sensor long inner readout sectors to their hybrids.

Table 2: Properties of the CMS-OB2 silicon sensors.

Bulk thickness	500 μm
Overall width	96.374 mm
Overall length	94.396 mm
Active width	93.869 mm
Active length	91.571 mm
Number of readout strips	512
Readout strip pitch	183 μm
Implant width	46 μm
Metal strip width	58 μm

The four-sensor long outer readout sectors are directly connected to their front-end readout hybrids via short pitch adaptors. The readout scheme is illustrated in Figure 2.

A cross section of the interconnect cable is shown in Figure 3. The cable is 391 mm long and carries 512 signal strips as well as two strips each for bias voltage and ground on a 100 μm thick Kapton substrate. A copper-mesh backplane provides a solid ground connection and shielding against pick-up noise.

An isometric drawing of the basic detector unit, consisting of seven silicon sensors, a Kapton interconnect, and two staggered front-end readout hybrids, is shown in Figure 4. The 14-sensor long ladders that cover the areas to the left and to the right of the beam pipe are assembled from two such detector units that are joined together.

A possible upgrade is illustrated in Figure 5. Here, the ladders close to the beam pipe are split into three readout sectors: an outer four-sensor long readout sector, an intermediate readout sector that is two sensors long and an inner readout sector consisting of a single silicon sensor. These ladders are equipped with three staggered front-end readout hybrids and two staggered Kapton interconnect cables. A standard 39.1 cm long Kapton cable connects the intermediate readout sector to its front-end hybrid, a second interconnect of the same cross section but 58 cm in length is employed for the inner readout sector.

Preliminary studies indicate that the finer segmentation in the central region of the detection layers, where particle densities are highest, may yield an improved Level-1 trigger performance. However, these studies have to be finalized before a decision on the segmentation can be taken. It should be noted that the finer segmentation is also advantageous for the signal-to-noise performance after irradiation since readout channels collect radiation-induced leakage currents from a smaller detector volume.

Compared to the original layout described in the TDR [1], the layout presented in this note offers several advantages:

- More sensible overlaps between adjacent ladders in the region above and below the beam pipe.
- A more sensible partitioning into readout sectors in the outer region of the detector where occupancy is low.
- The readout strip pitch is reduced from 198 μm to 183 μm.

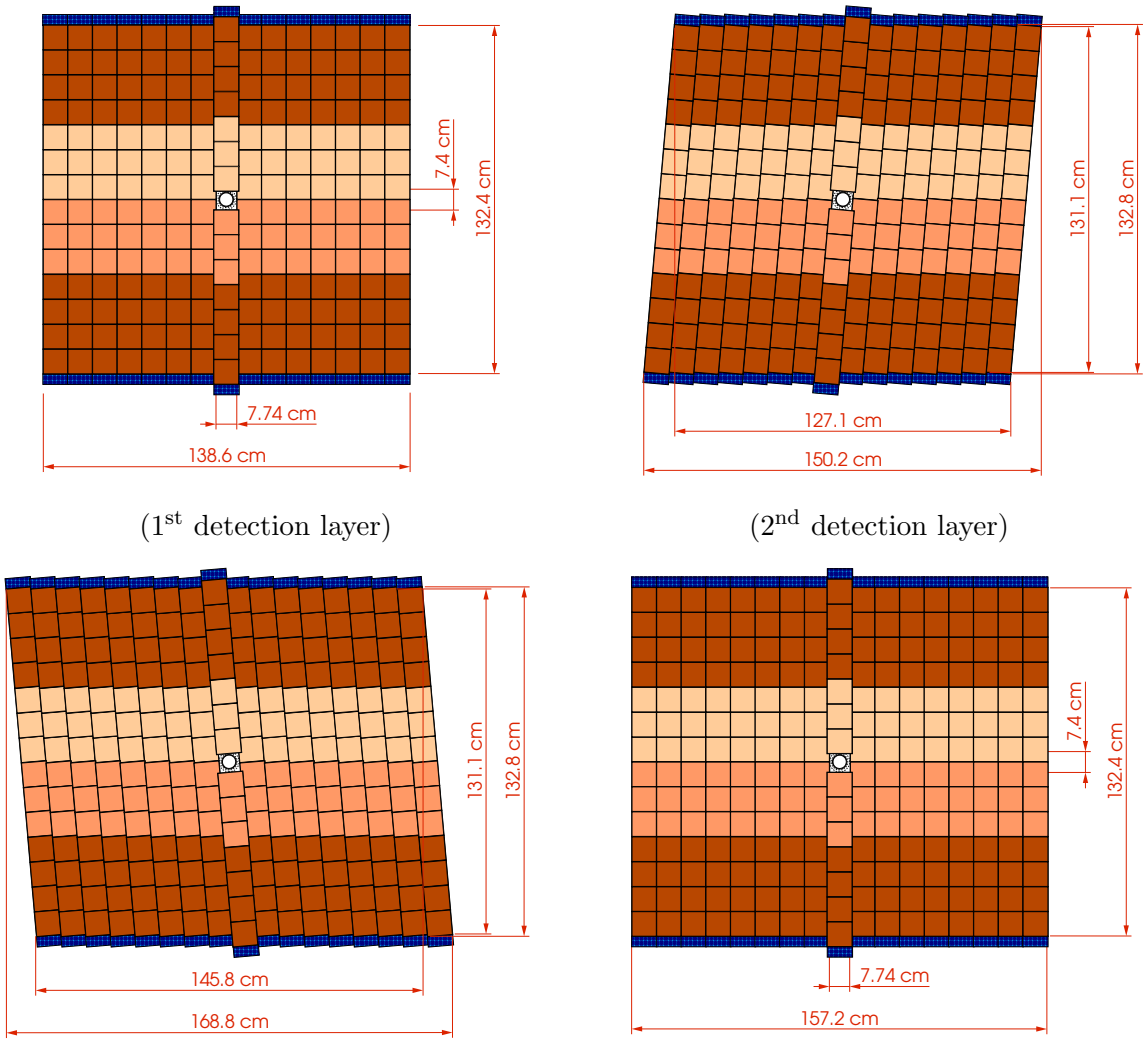

(1^{st} detection layer) (2^{nd} detection layer)

(3^{rd} detection layer) (4^{th} detection layer)

Figure 1: Layout of the four detection layers of the TT station. The different readout sectors along a silicon ladder are indicated by different shading.

- The possibility to build upon extensive experience and sensor R&D by the CMS collaboration.
- A significant reduction in the number of silicon sensors and readout channels.

The only disadvantage of the new layout is a slightly reduced acceptance coverage. The overall width of the active surface is 138.6 cm instead of the nominal 145.4 cm in the 1st detection layer and 157.2 cm instead of the nominal 162.1 cm in the 4th detection layer. Furthermore, the dead area in between two consecutive sensors on a ladder increases from 2.2 mm to 3.0 mm. This is due to a wider guard ring area on the CMS sensors than on the Inner Tracker sensors.

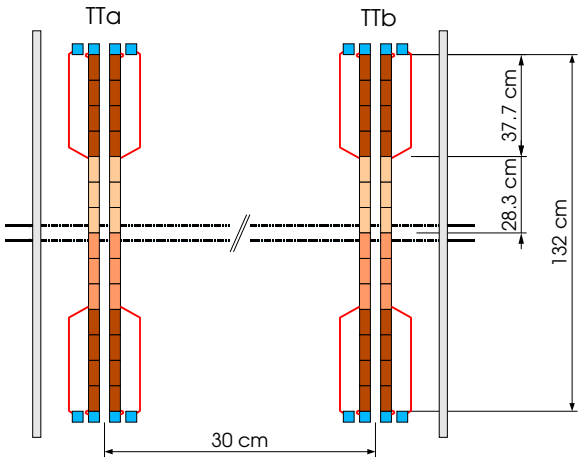

Figure 2: Sideview of the TT station, indicating the readout scheme with Kapton interconnect cables to read out the inner readout sector.

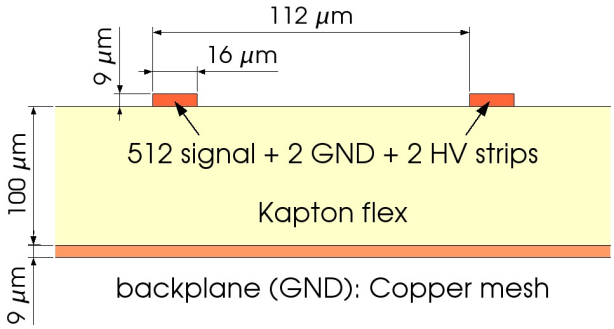

Figure 3: Cross section of the Kapton interconnect cable.

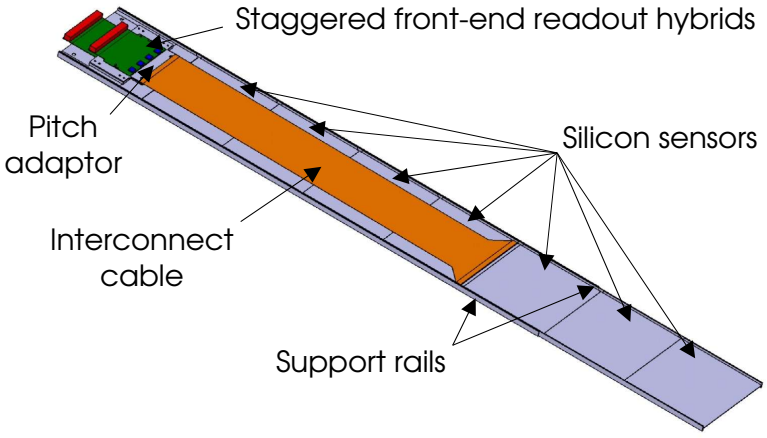

Figure 4: Isometric view of a TT half module, showing the two staggered readout hybrids and the Kapton interconnect employed to read out the inner readout sector.

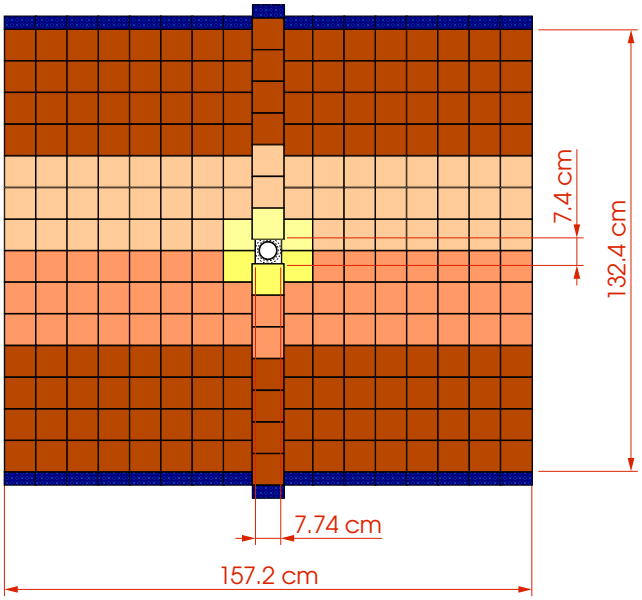

Figure 5: Possible upgrade for TT station, with three readout sectors for the innermost ladders around the beam pipe.

3 Strip Capacitances

The load capacitance at the input of the Beetle front-end pre-amplifier consists of contributions from strip capacitances on the silicon sensors, from the pitch adaptor, and the inner readout sectors from strip capacitances on the Kapton interconnect cable.

- The specific strip capacitance of the OB-2 silicon sensors has been measured to be 1.4 pF/cm [8]. This value is in good agreement with the result of a static ANSYS simulation.

- The total specific strip capacitance of the interconnect cable has been measured on a prototype to be 0.40±0.01 pF/cm. This result is in good agreement with a two-dimensional Maxwell simulation, which yielded a specific strip capacitance of 0.39 pF/cm.

- The capacitance of the pitch adaptor varies from 1 pF for readout strips in the middle of the sensor to 3 pF for channels close to the edge of the sensor.

In the calculation of total strip capacitances, a readout strip length of 9.44 cm was assumed for the CMS silicon sensors[2]. A capacitance of 2 pF was assumed for the pitch adaptor. Resulting total strip capacitances are summarized in Table 3, for the two readout sectors of the baseline layout ("4 sensor" and "3 sensor + cable") and for the two additional readout sector geometries employed in the upgrade ("2 sensors + cable" and "1 sensor + cable").

[2]This is a conservative assumption. As shown in Table 2, 9.44 cm is the physical length of the sensor whereas the length of the readout strips is 9.11 cm. The bond wires bridging the gap between the readout strips on two consecutive sensors in a readout sector should have a lower capacitance than the readout strips themselves.

Table 3: Total strip capacitances

readout sector	sensor length [cm]	cable length [cm]	capacitance [pF]
4 sensor	37.76	–	54.9
3 sensors + cable	28.32	39.1	57.3
2 sensors + cable	18.88	39.1	44.1
1 sensor + cable	9.44	58.0	38.4

Table 4: Noise performance of the Beetle 1.2 front-end readout chip (from [4])

V_{fs}	A_{ENC}	B_{ENC}
0 mV	790 e^-	50.3 e^- / pF
400 mV	776 e^-	47.9 e^- / pF
1000 mV	639 e^-	44.5 e^- / pF

4 Extrapolation Procedure and Expected S/N Performance

Measurements of the noise performance of the Beetle 1.2 readout chip as a function of load capacitance have been presented in [4] for different values of the signal shaping time of the front-end amplifier. The signal shaping time of the Beetle chip can be adjusted within a certain range by applying a control voltage V_{fs}. Larger values of V_{fs} correspond to longer signal shaping times and thus to a better noise performance. For a given setting of V_{fs}, the equivalent noise charge (ENC) of the chip was fitted by a linear function

$$\mathrm{ENC} = A_{\mathrm{ENC}} + B_{\mathrm{ENC}} \times C \text{ [pf]}.$$

The resulting values for the offset A_{ENC} and the slope parameter B_{ENC} for the three tested settings of V_{fs} are summarised in Table 4.

These results can be employed to scale the measured signal-to-noise performance of the tested prototype ladder to other readout strip lengths. The prototype ladder consisted of three CMS-OB2 sensors without Kapton interconnect cable, corresponding to a total readout strip capacitance of $C_{\mathrm{proto}} = 41.6\,\mathrm{pF}$.

An additional correction factor needs to be applied since the tests described in [4] were carried out using a 120 GeV π^- beam. Using the equations given in [5, 6], it is estimated that the most-probable value of the straggling function for 120 GeV $\pi^\pm$ is 7% higher than that for a minimium ionizing particle. Therefore, the predicted most probable signal-to-noise value $(S/N)_{\mathrm{on-strip}}$ for a ladder with total capacitance C_{tot} is given by:

$$(S/N)_{\mathrm{on-strip}} = 0.93 \times (S/N)_{\mathrm{meas}} \times \frac{A_{\mathrm{ENC}} + B_{\mathrm{ENC}} \times C_{\mathrm{proto}}}{A_{\mathrm{ENC}} + B_{\mathrm{ENC}} \times C_{\mathrm{tot}}}. \quad (1)$$

In all measurements, a significant charge loss has been observed for particles that pass the detector in the central region in between two readout strips. This leads to a worse signal-to-noise performance, which can be calculated using the following parameterization given in [4]:

$$(S/N)_{\mathrm{mid-strip}} = (A_{\mathrm{loss}} - B_{\mathrm{loss}} \times x_d) \times (S/N)_{\mathrm{on-strip}}.$$

where $x_d = (p - w)/t$, p is the pitch, w the implant width and t the sensor thickness. In [4], it was found that $A_{\rm loss} = 1$ and $B_{\rm loss} = 0.66$. For the geometry of the CMS-OB2 sensors, these values correspond to a charge loss of 12% (charge collection efficiency of 88%) in the central region in between two readout strips.

The extrapolated most probable signal-to-noise values for minimum ionizing particles are summarized in Tables 5, 6 and 7 for the three different settings of the Beetle shaping parameter $V_{\rm fs}$.

Also quoted in these tables is the corresponding signal remainder 25 ns after the maximum of the pulse, i.e. at the time of the next LHC bunch crossing. The most precise determination of this remainder as a function of shaping time and load capacitance was obtained in the laboratory setup, using an infra-red laser beam to generate charge in the prototype silicon ladders [7]. For a given signal shaping time, a roughly linear dependence of the signal remainder on the load capacitance was found and a first-order polynomial

$$\text{remainder} = A_{\rm rem} + B_{\rm rem} \times C \text{ [pF]}$$

was fitted to the measurements. The results of the fit for the three different settings of the Beetle shaping parameter $V_{\rm fs}$ are summarized in Table 8.

It should be noted that LHCb simulation studies show that the most probable value of $\beta\gamma$ for charged particles passing trough the TT station is 13. Such particles produce 3% higher signals than a minimum ionizing particle, which translates to 3% higher signal-to-noise values than those quoted here.

References

[1] *LHCb Reoptimized Detector Technical Design Report*, CERN-LHCC 2003-030

[2] *LHCb Inner Tracker Technical Design Report*, CERN-LHCC 2002-029

[3] J.-L. Agram et al., *The Silicon Sensors for the Compact Muon Solenoid Tracker — Design and Qualification Procedure*, CMS note 2003-015

[4] M. Agari et al., *Test-Beam Measurements on Prototype Ladders for the LHCb TT Station and Inner Tracker*, LHCb note 2003-082

[5] M. Needham, *Simulating Energy Loss in Thin Silicon Detectors*, LHCb note 2003-160

[6] H. Bichsel, *Straggling in Thin Silicon Detectors*, Rev. Mod. Phys. **60** 1988, 663-699

[7] R. Bernhard et al., *Measurements on Prototype Ladders for the Silicon Tracker with Laser*, LHCb note 2003-075

[8] J.Gassner et al., *Capacitance Measurements on Silicon Micro-Strip Detectors for the TT Station of the LHCb Experiment*, LHCb note 2003-081

[9] M. Agari et al., *Test-Beam Results of Multi-Geometry Prototype Sensorsfor the LHCb Inner Tracker*, LHCb note 2002-058

Table 5: Expected performance for $V_{fs} = 100\,mV$

readout sector	S/N on-strip	S/N mid-strip	remainder
4 sensor	14.5	12.8	34%
3 sensors + cable	14.1	12.4	35%
2 sensors + cable	17.2	15.1	27%
1 sensor + cable	19.0	16.7	25%

Table 6: Expected performance for $V_{fs} = 400\,mV$

readout sector	S/N on-strip	S/N mid-strip	remainder
4 sensor	15.1	13.3	44%
3 sensors + cable	14.6	12.8	45%
2 sensors + cable	17.7	15.6	38%
1 sensor + cable	19.7	17.3	35%

Table 7: Expected performance for $V_{fs} = 1000\,mV$

readout sector	S/N on-strip	S/N mid-strip	remainder
4 sensor	16.1	14.2	66%
3 sensors + cable	15.5	13.7	67%
2 sensors + cable	19.1	16.8	61%
1 sensor + cable	21.2	18.7	59%

Table 8: Parameters for the determination of the signal remainder (from [7]).

V_{fs}	A_{rem}	B_{rem}
0 mV	4.5%	0.53% / pF
400 mV	14.9%	0.53% / pF
1000 mV	42.1%	0.44% / pF

A Appendix: Expected Performance for TDR Layout

The same procedure as described in Chapter 4 has been applied to the TDR-layout of the TT station. Here, the largest load capacitance is 48.2 pF for the readout strips of the 3-sensor long outermost readout sector. The expected most probable signal-to-noise ratios for 410 μm thick sensors and for 500 μm thick sensors are listed in Tables 9 and 10, respectively. It can be seen from the results of the extrapolation, that in between readout strips the expected signal-to-noise performance for 410 μm thick sensors is only marginally better than the most probable value of ten that is required for full particle detection efficiency [9]. Robust operation of the detector cannot be ensured, especially taking into account that the signal-to-noise performance will further deteriorate with increasing irradiation dose received by the sensors.

Table 9: Expected performance for 410 μm thick sensors in the TDR layout.

V_{fs}	S/N on-strip	S/N mid-strip	remainder
0 mV	12.3	10.0	30%
400 mV	12.8	10.4	40%
1000 mV	13.7	11.1	63%

Table 10: Expected performance for 500 μm thick sensors in the TDR layout.

V_{fs}	S/N on-strip	S/N mid-strip	remainder
0 mV	16.1	13.0	30%
400 mV	16.7	13.5	40%
1000 mV	17.9	14.5	63%